Performances of endoscopic holography with a multicore optical fiber

Olivier Coquoz, Ramiro Conde, Fatemeh Taleblou, and Christian Depeursinge

A holographic setup that involves the use of a multicore optical fiber as an *in situ* recording medium has been developed. The hologram is transmitted to a CCD camera for electronic processing, and the image is reconstructed numerically, providing more flexibility to the holographic process. The performances of this imaging system have been evaluated in terms of the resolution limit and robustness relative to noise. The experimental cutoff frequency has been measured experimentally over a range of observation distances (4–10 mm) and presents a very good agreement with the predictions made by simulation. The system features a resolution of 5-μm objects for a 4-mm observation distance. The different sources of noise have been analyzed, and their influence on resolution has been proved to be nonrelevant.

Key words: Endoscopy, holography, multicore optical fiber.

1. Introduction

When combined with endoscopy, holography offers the physician additional diagnostic capabilities for observation of the cavities in the human body. Furthermore, profiting from technological progress in multicore fiber manufacturing, the recent development of miniaturized endoscopes, or microendoscopes, has permitted the exploration of very small channels of the body, such as coronary arteries, and has given rise to numerous medical interventions that are minimally invasive, or less invasive. Thus microendoscopic holography can lead to new medical applications, permitting the *in situ* microscopic imaging of tissues or deformation analysis.

The first development of endoscopic holography was performed more than 15 years ago.[1] It was shown at that time that a hologram could be recorded *in situ* with the use of a single-mode fiber for both the illumination and the reference beam. Another *in situ* holocamera was developed later to get *in vivo* three-dimensional photographic records of the vocal chords.[2] A special endoholoscope was then designed, in the single-beam Denisyuk configuration,[3] and was improved upon to reach a quasi-cellular resolution.[4] The main disadvantage of these setups is the inconveniences associated with the processing of the holographic film, which is placed at the distal tip of the endoscope and must be changed after each exposure.

Other groups used the so-called external recording technique, in which the object wave interferes with the reference at the output of the endoscope. This setup was applied to the investigation of the tympanic membrane vibration patterns with a rigid endoscope[5] and to the measurement of remote deformations with a flexible endoscope.[6] It was demonstrated that endoscopic holography could achieve three-dimensional imaging as well as interferometric analysis of an organ inside the body.[7]

In the *in situ* holographic technique presented here, we keep the advantage of internal recording, i.e., phase conservation to form the hologram, while getting rid of its main drawback, which is the use of the holographic plate and its relatively complex handling. In our setup the hologram is collected on the tip of the multicore optical fiber (MCF),[8] in a quasi on-axis setting, and transmitted to a CCD camera for acquisition. Eventually the reconstruction is performed numerically,[9,10] adding in this way more flexibility to the holographic process and offering new solutions to solve difficult experimental problems.[11]

The first objective of our study was to evaluate the performance of the miniaturized endoholoscope. A simulation program of the entire Fresnel holographic process was developed to predict the resolution limit as a function of the different parameters involved. Experimental measurements performed under the conditions matched by the simulation fully confirmed the theoretical predictions. Further-

The authors are with the Applied Optics Laboratory, Swiss Federal Institute of Technology in Lausanne, CH-1015 Lausanne, Switzerland.

Received 13 October 1994; revised manuscript received 30 May 1995.

0003-6935/95/317186-08$06.00/0.

more, the different sources of noise encountered experimentally were analyzed and their influence on the resolution limit was evaluated. The commonly observed speckle noise is not discussed here; it should be minimized in our experiments, because of the absence of parasitic scattering centers. Indeed, the use of the standard U. S. Air Force positive test target as an object prevents speckle originating from multiply scattered light. Noise caused by multimodal propagation of light in the MCF and by its weak guiding properties was investigated. The importance of this noise was compared with the observed structural noise, which seems to be the main cause of signal degradation.

2. Materials and Methods

Our holographic images result from a hybrid numerical-experimental method. Its main features are the *in situ* hologram recording on the distal extremity of a MCF, and the fully numerical image reconstruction (Fig. 1). It offers the possibility of getting rid of the problems related to photographic plate processing, and it permits a convenient and high-performance means to control electronically the wave-front reconstruction. The limiting factors of our setup and the particular conditions of the hologram recording have been the objects of our study. In particular, the influence of the low density of our recording system has been investigated, as well as the behavior of the resolution limit when the observation distance is varied. A formalism was then defined to evaluate the resolution, by derivation of the transfer function of the system, in the case of coherent illumination. We call this function the amplitude modulation transfer function (AMTF) to take into account that a coherent imaging system is linear in the amplitude of the electromagnetic field.

A. Simulation

The developed miniaturized endoholoscope is used for coherent imaging at a microscopic level, and the observations are performed in the near-field (Fresnel) diffraction region, typically at distances in the range of a few millimeters.

Following the theory formulated for Fresnel-type holography,[12] we can write the hologram intensity as

$$I_H = |H|^2 = |O + R|^2 = |O|^2 + |R|^2 + O^*R + OR^*, \tag{1}$$

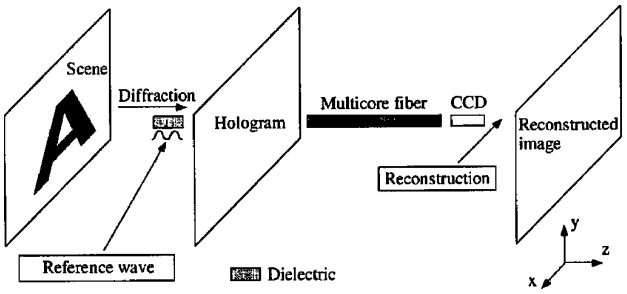

Fig. 1. Schematic arrangement of the holographic setup.

where O is the object wave, R is the reference, and H is the total field observed. The third and fourth terms in this expression are the interference terms, which form the real and virtual images, respectively, after reconstruction. Considering a planar object, we can express the wave-field amplitude in the hologram plane as the sum of the wavelets emitted from all the points of the object characterized by the amplitude distribution of light, $U_o(x_o, y_o)$. In the Fresnel approximation it can be written as

$$O(x, y) = A \int_{\text{object}} \int U_o(x_o, y_o) \times \exp\left\{\frac{ik}{2z_o}[(x_o - x)^2 + (y_o - y)^2]\right\} \mathrm{d}x_o \mathrm{d}y_o. \tag{2}$$

This expression describes the Fresnel transform of the object defined by distribution $U_o(x_o, y_o)$, located at a distance z_o from the hologram, where A is a complex constant. The expression for the reference wave is obtained in a similar fashion: in our setup, it is provided by a single-mode fiber (SMF) illumination, the phase term of which can be considered as spherical in the range of distances investigated.

The geometrical setup was chosen with a small angle so that the hologram fringes present a low-frequency pattern. Indeed, the recording system includes a MCF to sample and transmit the hologram; this MCF has a cutoff frequency much lower than that of the usual holographic plates, i.e., $\sim$100 lp/mm (line pairs/mm) versus $\sim$1000 lp/mm. The best way to avoid the low-pass filtering caused by multicore fiber sampling is to use on-axis geometry, but its drawback is the superposition of the twin images on the same axis. The quality of the reconstructed image is significantly reduced by this twin-image problem, which can be eliminated or attenuated by different proposed techniques, even those by Gabor himself.[13] To avoid this artifact, we have chosen an angular arrangement such that the reconstructed image is separated from the background light produced by the direct transmission of the illumination beam through the hologram.

Usually one reconstructs a hologram by illuminating it with a wave similar to the reference. Here we perform the reconstruction numerically by calculating the Fresnel diffraction of the illuminated hologram in a given plane, in other words, by computing its Fresnel transform at a certain distance.[9,10] The reconstructed image will be focused when the value chosen matches the distance at which the object was observed. The Fresnel transform operation consists of the convolution with the chirp function:

$$\mathrm{ch}(x, y) = \frac{1}{z} \exp\left[\frac{ik(x^2 + y^2)}{2z}\right]. \tag{3}$$

By this computation, we obtain the diffracted image

in a plane located at a distance z from the hologram. Using the indirect method for convolution (by means of Fourier transform), we found the algorithm to be fast and appropriate for this problem. It was used for the reconstruction of experimental holograms.

The simulation of the whole process (recording and reconstruction) was performed to predict the resolution of our system, according to the Fresnel diffraction theory. The main parameters to be considered are the multicore fiber density, aperture, and observation distance. The spatial resolution is often characterized by the frequency analysis of the imaging system. In our simulation, we consider as our object an ideal point source (Dirac); then the hologram is formed when its diffracted image is combined with a spherical reference wave. The object and reference directions form a very small angle θ. To perform the reconstruction, we use a wave identical to the reference as illumination of the hologram; then we obtain the image by computing the Fresnel transform of the wave front going out of the hologram in the direction θ. This image is nothing but the impulse response of our system, or point spread function. Because we are working with coherent imaging, the frequency analysis has to be applied on the complex amplitude of the field,[14] and we will systematically add the word amplitude as a prefix to the function names as a reminder. Therefore, we can derive the coherent or amplitude transfer function by achieving the Fourier transform of the amplitude point spread function. The modulus of the ATF is referred to here as the AMTF. The cutoff is defined for a frequency, the AMTF corresponding value of which is equal to one half of the amplitude, to obtain a signal-to-noise ratio of 10.[15]

B. Experiments

A miniaturized flexible endoscope imaging multicore fiber (Fujikura FIGH-10-510N, 0.46-mm imaging diameter, 10,000 cores) was used for *in situ* holographic recording (Fig. 2). The angle between the object and reference directions was minimized to reduce the density of fringes in the hologram. Illumination was provided by a SMF with a monomodal transmission at a wavelength of 633 nm (He–Ne laser source). The reference beam was produced by partial reflection on an optical flat used as a beam splitter, slightly tilted so that the reflected beam was centered on the MCF placed beside the SMF. The tilt angle was approximately 6.5°. For the interference of the light reflected on both interfaces of the optical flat to be minimized, the front interface received an antireflection coating (Fig. 3). In this case, only the light incident on the back panel is reflected. The light reflected by the object interferes with the reference beam to form the hologram on the MCF tip. It is sampled and transmitted by each individual fiber core of the MCF to a CCD camera for digitization.

The reconstruction was performed numerically with an algorithm described in Subsection 2.A, which uses a Fresnel transform to reconstruct the focused image of the illuminated hologram. With this type of procedure, both the recorded hologram and the reconstructed image can be treated electronically to eliminate the background illumination and accentuate contrast and contour.

The key point for a good numerical reconstruction is the ability to reproduce as accurately as possible the reference beam in the hologram illumination step. Particularly, as expected, the phase distribution must be carefully computed to match the reference so that propagation and focusing of the reconstructed image are performed in the same conditions as during the recording process. This point is especially important when holography is realized with spherical waves, as in our case. SMF illumination (NA $\cong$ 0.1) was found to be a good solution to build the first prototype for two reasons. First, it is convenient to assemble in the experimental setup; second, both the phase and amplitude of the light beam launched at its output can be easily and reliably quantified.

The experiments were performed with a planar object, namely, the U. S. Air Force (USAF) positive test target. This standard test object contains horizontal and vertical three-bar patterns, characterized by 1–228-lp/mm, spatial frequencies in the form of a reflecting chromium coating set on a BK-7 glass substrate. The glass substrate was antireflection coated to ensure that the object wave information comes only from the chromium bar patterns.

The experimental AMTF is defined by the normalized amplitude contrast measurement,

$$\mathrm{AMTF} = \frac{A_{\max} - A_{\min}}{A_{\max} + A_{\min}}, \tag{4}$$

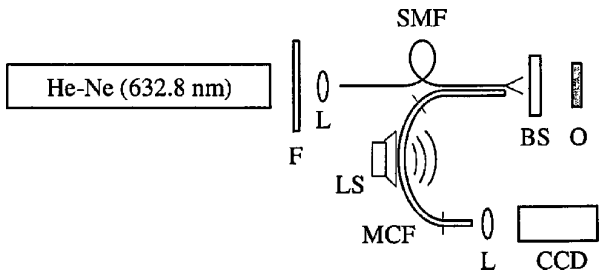

Fig. 2. Experimental setup: F, the neutral-density filter; L, lens; BS, beam splitter; O, object; LS, loudspeaker.

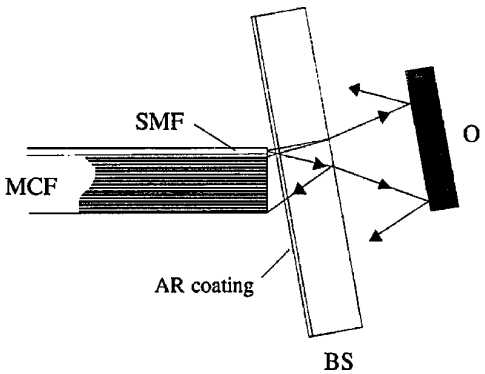

Fig. 3. Detail of the distal part of the experimental setup; AR, antireflection; BS and O, as defined in Fig. 2 caption.

where A_{max} and A_{min} stand for maximal and minimal values of the field amplitude in the reconstructed image. We could evaluate the spatial resolution of our system, by systematically deriving the cutoff frequency from the measured AMTF, for different observation distances and compare it with predictions given by simulation.

Holograms recorded with our setup suffer degradation introduced mainly by the MCF. Indeed, the MCF produces three kinds of noise when used with coherent light. The first is structural noise, induced by the nonuniform light coupling in each individual core caused by morphological inhomogeneities of the MCF. The second is caused by cross talk between adjacent cores and recoupling of leaky modes in a core. The third is interference between modes within a core, introduced by the multimodal characteristics of light propagation in the multicore fiber.[16,17]

The importance of cross talk was investigated experimentally in the following way: a laser beam was focused on a single core at the input of the MCF. The light intensity was then carefully measured at the output of the MCF with a photodiode as a reference to determine precisely the coupling between adjacent and distant cores.

Modal noise, caused by the interference of modes propagating in each individual core of the multicore fiber, appears as an additional disturbing effect. The experimental setup designed to attenuate this noise made use of a loudspeaker to apply a slight deformation to the MCF (Fig. 2), modifying the path length traveled by the light in each core. Interference between modes traveling in a single core is altered as well, and if a vibration frequency higher than the video sampling rate is applied, the captured image shows an averaged light intensity transmitted by the fiber core. This manipulation provokes a noise reduction in the fringes so that they become clearly distinct. Of course, each extremity is tightened to avoid any parasitic blurring effect caused by movement. We could, by comparing raw and vibrated images, isolate the modal noise, analyze it, and see whether it has an influence on spatial resolution.

Noise analysis was performed according to the following procedure: the image of the MCF section was first segmented with an ad hoc program. A calibration image, obtained by the illumination of the MCF with uniform white light, was used to define the position and surface associated with each core. Light intensity transmitted by each individual core could then be quantified, providing the base for a statistical analysis of the image distortion caused by the nonuniform light coupling in the fiber cores and cross talk. The same computer-assisted analysis was performed on images of MCF illuminated with a uniform coherent light source (He–Ne laser, 633 nm). The mean intensity transmitted by each core was obtained by an integral weighted over its surface. The variance of the core intensity histogram provides quantitative information on the noise influence, including modal noise as well. The importance of the different noise sources was compared on the basis of the coefficient of variation, i.e., the ratio of the variance to the signal mean.

3. Results

Typical results obtained with our hybrid experimental-numerical method are illustrated in Fig. 4. A hologram of USAF test target patterns (elements of group 6) is shown, after digitization on a CCD. Here the contribution of the reference wave intensity [second term in Eq. (1)] is subtracted to enhance the fringe visibility. The corresponding numerically reconstructed image shows that the patterns could be resolved with good quality up to 102 lp/mm at a distance of 4 mm.

Our microendoscopic system was capable of restoring three-dimensional information of the observed object by locating the plane where the reconstructed

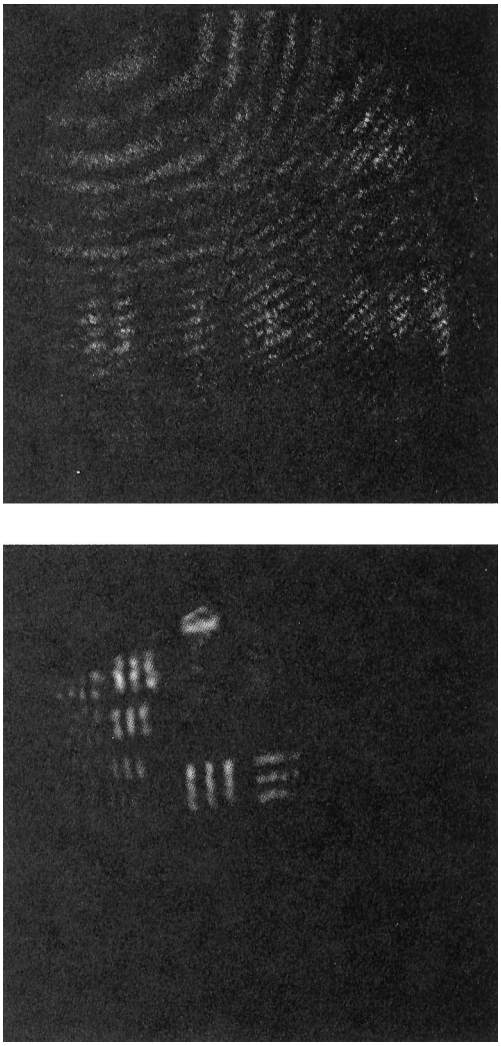

Fig. 4. Top, hologram of USAF test target patterns (elements of group 6) collected on the MCF and digitized on a CCD camera. Bottom, the focused reconstructed image shows patterns of frequency of 64 lp/mm (vertical and horizontal patterns at right), and 80.6, 90.5, 102, and 114 lp/mm (vertical patterns top to bottom at left). The observation distance was 4 mm.

image was focused (Fig. 5). Precise measurement of the observation distance to the object was rendered possible by the use of a micrometric translation stage to move the object and the miniaturized endoholoscope prototype. A calibration of the distance was necessary before the measurement was acquired. Nevertheless, one has to be careful with the use of this distance in the calculation because the light travels through two different media (air and quartz), characterized by two different wave numbers. Furthermore, the tilt angle of the optical flat influences the spatial distribution of the interference fringes. These factors must be considered when the phase and amplitude data of the reference beam are introduced in the image reconstruction procedure of the hologram and in the determination of the reconstruction distance with the focusing condition.

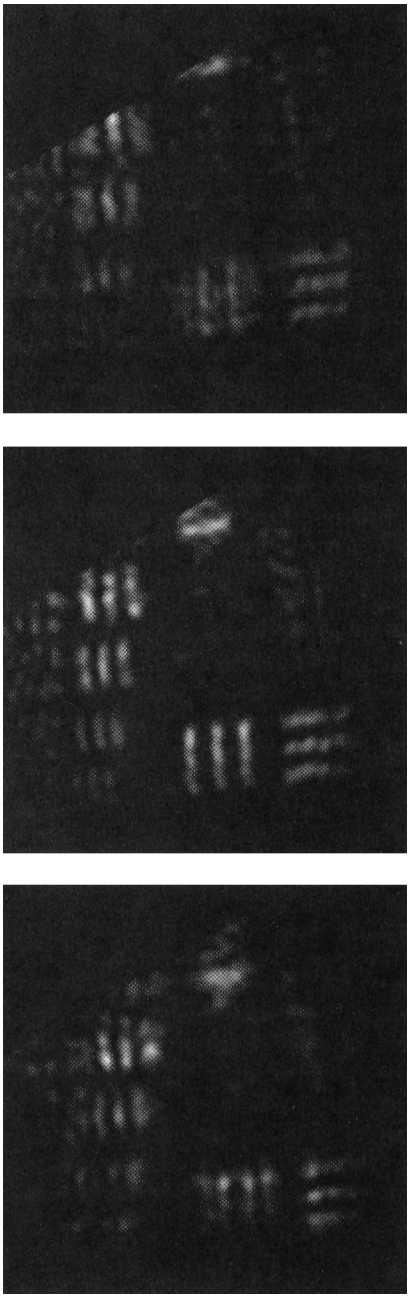

Fig. 5. From top to bottom, the image reconstructed at $d - 0.15$ mm, d, and $d + 0.15$ mm, respectively. These images illustrate the capability of our system to restore three-dimensional information by focusing the reconstructed image with a precision of less than 0.15 mm for an observation distance of $d = 4$ mm.

Measurements on the USAF test target were performed for different distances so that the cutoff frequency could be systematically determined and compared with the simulation predictions. The experimental AMTF could be derived from contrast measurements and plotted along with the simulated AMTF (Fig. 6). The results obtained from the simulation show some oscillations caused by numerical artifacts, coming from the windowing effect occurring in the Fourier transform computations involved in the algorithm. The main information concerning the resolution power is given by the cutoff frequency derived from the transfer function. A criterion for cutoff at an AMTF value of one half (signal-to-noise ratio of 10) was stated previously (Subsection 2.A). However, we have noticed in our systematic observations that patterns could be clearly distinguished even when they had an amplitude contrast measured below the one-half threshold. Therefore, to provide information that better corresponds to what the observer can see with this technique, we applied a lower requirement to the determination of cutoff frequency, i.e., an AMTF value of 0.25. It is critical to note that this value does not guarantee a high signal-to-noise ratio value of the reconstructed object signal. The experimental cutoff frequency was compared with the simulation in the same conditions and with the same criterion, over a range of observation distances (Fig. 7), and it showed good agreement.

One of the principal anticipated outcomes of the simulation predictions was to evaluate the importance of low-pass filtering because the hologram had to be sampled on the MCF tip, presenting a linear core density of $\sim 200\ \text{mm}^{-1}$, which should permit a correct sampling up to 100 lp/mm. Logically, if we stand far enough from the object, the limit is due to the multicore fiber aperture, which cuts the higher-

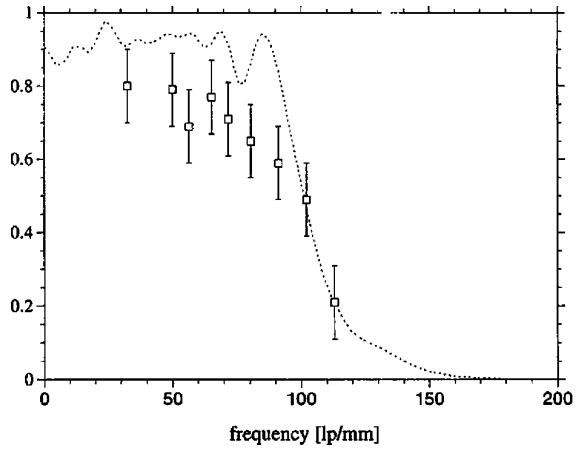

Fig. 6. Simulated (dashed curve) and experimental (squares) AMTF at 4-mm distance.

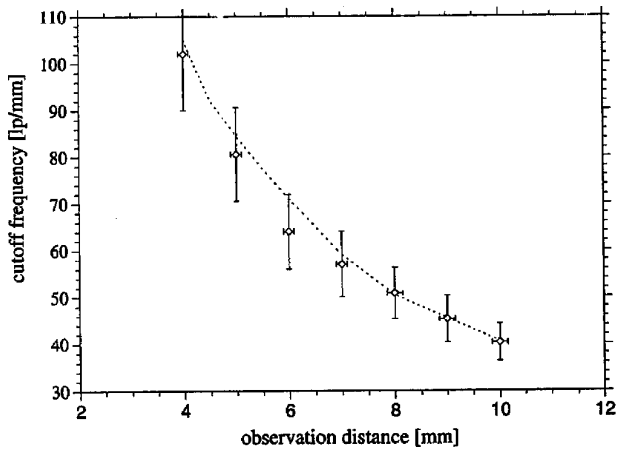

Fig. 7. Cutoff frequency versus observation distance, calculated by simulation (dashed curve) and derived experimentally (diamonds).

frequency hologram fringes. When we get closer to the observed object, the hologram fringes are more dense and can no longer be sampled correctly over the whole surface of the multicore fiber, which is then the limiting factor for resolution. Therefore, the behavior of the resolution power will be governed by the multicore fiber density, imposing a limit for the cutoff frequency at small observation distances, and by aperture for larger distances, with a hyperbolic decrease (Fig. 8). This behavior was in fact verified by simulation with a simulated multicore fiber featuring a perfectly hexagonal arrangement.[18] However, the arrangement of cores in the MCF is rather random. This permits an oversampling of the signal by the MCF, resulting in a cutoff not as distinctly observed as expected. As we get closer to the object the hologram fringes are no longer sampled accurately by all the MCF cores, already inducing a loss of signal for the frequencies below cutoff. This phenomenon begins at observation distances under 2 mm (Fig. 9). Finally, MCF sampling is responsible for a large attenuation of AMTF values, qualifying it definitely as the most limiting factor for observations closer than 1.5 mm. These results were obtained by simulation of the hologram sampling on an actual experimental image of an MCF. Unfortunately, these two different parts of the cutoff frequency curve could not be demonstrated experimentally because of the technical limits of our prototype. All the measurements were performed in a range of distances ($d \geq 4$ mm) in which the multicore fiber density effect on resolution is negligible.

Experiments were performed to analyze and quantitatively characterize the different sources of noise. Interference effects between the different modes of propagation in a fiber core could be evaluated by comparison of an image recorded in normal conditions to an image in which vibration applied to the imaging multicore fiber provoked an averaging of the light pattern transmitted by the cores (Fig. 10). The noise is not totally eliminated, but its drastic reduction smooths the signal shape, and allows, for instance, the human eye to read better the fringes of the hologram. This is explained by the fact that, in the presence of vibration, light transmitted by each core is distributed over several propagation modes, leading to a spreading of the intensity shape. The light globally transmitted by an individual core could be altered by 10–20%, depending on the bending radius or the vibration applied to the MCF. This variation is due to the cross talk and the coupling of radiative modes, acting mostly between adjacent cores. Our experimental observations have shown that ~15% of the light focused into a single core (fundamental mode) could be coupled in adjacent cores. We could also demonstrate that the total intensity transmitted by the MCF remains constant, reinforcing our statement that these local intensity variations are due to interaction phenomena between adjacent cores, and even between different propagation modes within the same core. As a major result, we have been able to verify, both experimentally and by simulation, that

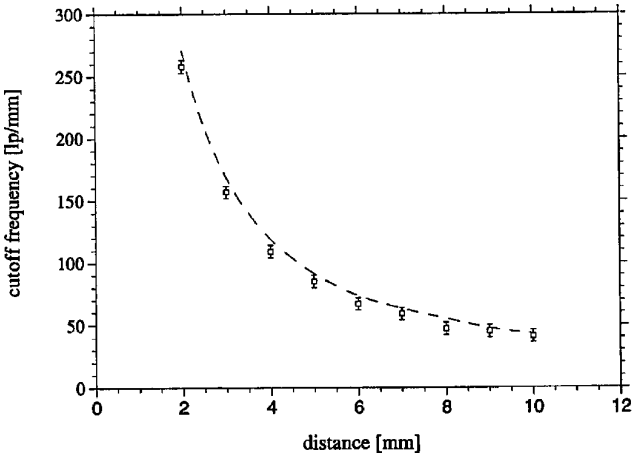

Fig. 8. Plot of the cutoff frequency as a function of observation distance, showing the effect of sampling the hologram on the MCF (squares) and the limitation caused by the aperture only (dashed curve).

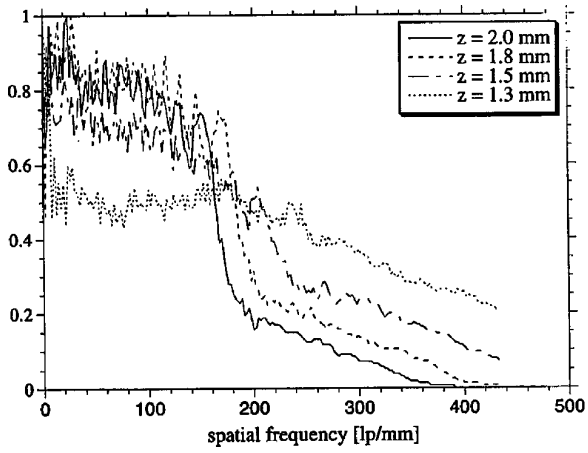

Fig. 9. Plot of the simulated AMTF's for different observation distances ($z \leq 2$ mm), showing a decrease of the AMTF level for frequencies below cutoff caused by nonoptimal fringe sampling by the MCF.

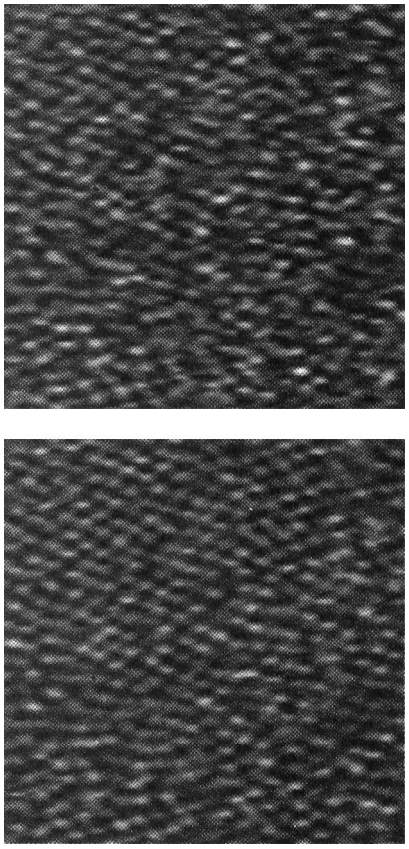

Fig. 10. Images showing a uniform coherent signal transmitted through stable (top) and vibrated MCF (bottom).

this noise does not influence the resolution limit significantly. This result, surprising at a first glance, can be explained: information carried by the interference fringes is disturbed only locally, so we take advantage of the statistical averaging to retrieve it from the noise. Furthermore, the modal noise has a spatial frequency content higher than that of the holographic signal. In this case, the information necessary for reconstruction is not altered significantly, as far as resolution is concerned.

Finally, the most important perturbation to the signal is due to structural noise. Indeed, the light coupling into the multicore fiber is strongly dependent on the core morphology. This effect is enhanced when coherent light is used, compared with white light for which the intensity is supposed to be distributed among the whole set of propagation modes of the core.

The relative importance of all the different sources of noise described above was investigated quantitatively by application of a uniform signal at the entrance to the MCF. The signal mean and standard deviation were measured at the output of the multicore fiber under three different conditions, i.e., with incoherent light, or with coherent light with or without vibration applied to eliminate multimodal interference effects. The ratio of standard deviation to signal mean gives information on the heterogeneity of the output signal introduced by the MCF noise. The influence of noise introduced by the MCF to the hologram on the reconstructed image was quantified. The coefficient of variation was shown to be approximately of the same order as noise in the hologram. Furthermore, in the absence of MCF sampling, there is intrinsic noise caused by numerical artifacts. Indeed, the image of a uniformly intense object is reconstructed with a fluctuation characterized by a variance of 9% of the signal mean, without the MCF noise. Table 1 shows that structural noise is important in the case of coherent illumination, whereas modal noise, although it is very remarkable by visual perception, adds only ~10% of intensity spreading, compared with the structural noise component.

4. Discussion

The possibility of using a numerical holographic reconstruction seems to be a valuable approach toward the development of holography in different applications. The numerical modeling of Fresnel holography has proved to be adequate, and its results have been successfully verified experimentally. However, we need to be aware of numerical artifacts, such as the windowing effect, which prevent us from obtaining a wide uniform field of reconstruction. The algorithm chosen was quite simple and allowed us to foresee that it could lead to quasi real-time image reconstruction, with the help of a digital signal processor and its associated software.[11]

The experimental research involving the evaluation of the amplitude MTF suffered a lack of precision in the cutoff slope definition. This was due to the fact that measurements were made only with one object, the USAF target, which offers a limited number of frequency patterns. Other standard test objects were examined but were found to be inadequate for holography. Ronchi rulings available for our experiments did not feature a smooth surface, and a variable frequency test target[19] induced a parasitic grating effect that disturbed the real focused image. The most promising result was the resolution of micrometric objects (5 μm) with a low-frequency recording medium, i.e., the MCF. This resolution is comparable with what was obtained before with holographic plates (4.38 μm) under different experimental conditions.[4] This establishes the possibility of microscopic coherent imaging of biological tissues at the cellular level, which is a major advantage of this method.[4] This performance is very attractive for future possible medical applications, because it signifi-

Table 1. Noise Statistics: Coefficient of Variation (Ratio of Variance σ to Signal Mean μ) for the Hologram and Reconstructed Image

	σ/μ (%)	
Experimental Condition	Hologram	Reconstructed Image
Incoherent illumination	11	10
Coherent illumination	28	24.5
Coherent illumination, vibration applied to MCF	25	23

cantly improves the resolution achievable in conventional microendoscopy. Furthermore, the versatility introduced by the electronic processing of the holographic image is an undeniable asset for its use in routine procedures by the physician. The minor role played by the MCF in the resolution limitation should encourage the use of holographic recordings in medical applications without the help of holographic plates. This extends the potential use of the holographic technique to new domains of investigation. The quality of the hologram endoscopic recording could be greatly improved with technological advances, and no longer suffers the drastic limitations encountered by the group who first experimented with this method.[8] The results obtained in the quantitative analysis of noise have revealed that the spatial resolution obtained with our method is not sensitive to perturbations introduced by different phenomena occurring in the MCF transmission. In particular, the noise produced by modal interference in each core, which seemed to be important following the first visual observations, turned out to be unimportant for the resolution capabilities of our endoholoscope. Structural noise contribution was shown to be the major perturbation to the signal, and it is an unavoidable drawback to the use of an endoscope with coherent light. The quantitative analysis of intensity fluctuations in the reconstructed image showed that the detectability of the signal can be perturbed by the noise coming from the MCF. However, this was not a major drawback in the measurements performed because the USAF target elements presented an optimally contrasted signal. Finally, these different noise sources do not significantly affect the resolution power of our system. This is the major conclusion of our analysis.

5. Conclusion

The method of applying a numerical reconstruction procedure to experimental holograms has been successfully demonstrated in the conditions of miniaturized endoholoscopy. The resolution performances obtained with our experimental setup have shown a very good agreement with the predictions obtained by simulation, based on the Fresnel diffraction modeling. The identification of 5-μm objects for a 4-mm observation distance has been possible and let us foresee the imaging of biological tissues at the cellular level. The analysis of the different sources of noise allowed a detailed understanding of the phenomena occurring in our processing but evidenced no relevant resolution loss caused by these perturbations. This can be seen as a robust property of this holographic method toward experimental defects. This research indicates that the method is feasible and opens a new way to what could be called numerical microholography, which brings new and attractive perspectives to the study of the morphology of very small organs and cavities as well as tissues even at the cellular level.

This research was supported by the Swiss Priority Program in Optics, CEPF-PPO/MED. The authors thank E. B. de Haller for his important contribution to the experimental setup, G. von Bally for fruitful discussions, and R. and N. Croisy (Andromis Ltd., Geneva) for constant interest.

References

1. D. Hadbawnik, "Holographische endoskopie," Optik **45,** 21–38 (1976).
2. G. Raviv, M. E. Marhic, E. F. Scanlon, S. F. Sener, and M. Epstein, "*In vivo* holography of vocal chords," J. Surg. Oncol. **20,** 213–217 (1982).
3. H. I. Bjelkhagen, M. D. Friedman and M. Epstein, "Holographic high resolution endoscopy through optical fibers," Proc. Laser Inst. Am. **64,** 94–103 (1988).
4. H. I. Bjelkhagen, J. Chang, and K. Moneke, "High-resolution contact Denisyuk holography," Appl. Opt. **31,** 1041–1047 (1992).
5. G. von Bally, "Otoscopic investigations by holographic interferometry: a fiber endoscopic approach using a pulsed ruby laser system," in *Proceedings of the International Conference on Optics in Biomedical Sciences,* G. von Bally and P. Greguss, eds. (Springer-Verlag, Berlin, 1982), pp. 110–114.
6. J. A. Gilbert, T. D. Dudderar, and A. Nose, "Remote deformation field measurement through different media using fiber optics," Opt. Eng. **24,** 628–631 (1985).
7. H. Podbielska and A. Friesem, "Endoscopic optical metrology—the possibilities of holographic interferometry," in *Optical Fibers in Medicine V,* A. Katzir, ed., Proc. Soc. Photo-Opt. Instrum. Eng. **1201,** 552–560 (1990).
8. T. D. Dudderar, J. A. Gilbert, and A. J. Boehnlein, "Achieving stability in remote holography using flexible multimode image bundles," Appl. Opt. **22,** 1000–1005 (1983).
9. W. S. Haddad, D. Cullen, J. C. Solem, J. W. Longworth, A. McPherson, K. Boyer, and C. K. Rhodes, "Fourier-transform holographic microscope," Appl. Opt. **31,** 4973–4978 (1992).
10. U. Schnars and W. Juptner, "Direct recording of holograms by a CCD target and numerical reconstruction," Appl. Opt. **33,** 179–181 (1994).
11. E. Leith, C. Chen, H. Chen, Y. Chen, D. Dilworth, J. Lopez, J. Rudd, P. -C. Sun, J. Valdmanis, and G. Vossler, "Imaging through scattering media with holography," J. Opt. Soc. Am. A **9,** 1148–1153 (1992).
12. H. M. Smith, *Principles of Holography* (Wiley, New York, 1975), Chap. 3.
13. D. Gabor and W. P. Goss, "Interference microscope with total wavefront reconstruction," J. Opt. Soc. Am. **56,** 849–858 (1966).
14. J. W. Goodman, *Introduction to Fourier Optics* (McGraw-Hill, San Francisco, Calif., 1968), Chap. 6.
15. J. B. DeVelis and G. O. Reynolds, "Fresnel holography," in *Handbook of Optical Holography,* H. J. Caulfield, ed. (Academic, New York, 1979), pp. 139–155.
16. W. B. Spillman, B. R. Kline, L. B. Maurice, and P. L. Fuhr, "Statistical-mode sensor for fiber optic vibration sensing uses," Appl. Opt. **28,** 3166–3176 (1989).
17. C. O. Egalon and R. S. Rogowski, "Model of an axially strained weakly guiding optical fiber modal pattern," Opt. Eng. **31,** 1332–1339 (1992).
18. O. Coquoz, C. Depeursinge, R. Conde, and F. Taleblou, "Performance of on-axis holography with a flexible endoscope," in *Holography, Interferometry, and Optical Pattern Recognition in Biomedicine III,* H. Podbielska, ed., Proc. Soc. Photo-Opt. Instrum. Eng. **1889,** 216–223 (1993).
19. Edmund Scientific Company, Barrington, N.J. 08007-1380.